Characterization of malignant tissue cells by laser-induced breakdown spectroscopy

Akshaya Kumar, Fang-Yu Yueh, Jagdish P. Singh, and Shane Burgess

Cancer diagnosis and classification is extremely complicated and, for the most part, relies on subjective interpretation of biopsy material. Such methods are laborious and in some cases might result in different results depending on the histopathologist doing the examination. Automated, real-time diagnostic procedures would greatly facilitate cancer diagnosis and classification. Laser-induced breakdown spectroscopy (LIBS) is used for the first time to our knowledge to distinguish normal and malignant tumor cells from histological sections. We found that the concentration of trace elements in normal and tumor cells was significantly different. For comparison, the tissue samples were also analyzed by an inductively coupled plasma emission spectroscopy (ICPES) system. The results from the LIBS measurement and ICPES analysis were in good agreement. © 2004 Optical Society of America

OCIS codes: 140.3440, 170.6930, 300.2140, 300.6210, 300.6360.

1. Introduction

Different techniques are practiced to identify malignant from nonmalignant tissue cells. Although much cancer research now focuses on the fundamental molecular pathology of cancers, a critical applied clinical issue remains the early, rapid, and accurate diagnosis of cancer so that complete surgical removal of that cancer can be effected. Some diagnostic techniques distinguish different proteins, whereas others rely on identifying abnormal cellular morphology. Most recently, transcriptomics and proteomics are being developed to identify gene expression profiles diagnostic of malignancy. Complementary DNA microarrays and serial analysis of gene expression are used for transcriptomics and two-dimensional gel electrophoresis[1]; matrix-assisted laser desorption ionization mass spectroscopy[2,3] and surface-enhanced laser desorption ionization mass spectroscopy[4] are used for proteomics. All these techniques have the common disadvantages of being time-consuming, expensive, and requiring a relatively complicated sample preparation. Other techniques, such as x-ray fluorescence and proton-induced x-ray fluorescence, monitor the concentrations of nutrient metal ions, which are different in malignant and nonmalignant cells.[5–7] However, x-ray fluorescence is a technique used for elemental analysis for the element with an atomic number above 8. It cannot readily detect the common elemental constituents of organic materials such as carbon, hydrogen, oxygen, and nitrogen. Laser-induced breakdown spectroscopy (LIBS) is a developing and promising technology that has the advantages of simplicity and robustness.[8–12] It can detect the elemental constituent in both low and high atomic number elements. In LIBS, a pulsed laser light is focused on the sample to create the breakdown and spark of material, and the light emitted in the spark is analyzed by a spectrometer. Unique features of LIBS are its on-line capability where composition of the material can be analyzed in a fraction of a second without any sample preparation. A wide range of studies that used the LIBS technique have been carried out in all kinds of samples, i.e., solids, liquids, and gases. LIBS has been used in biology.[13–20] Yet LIBS has never been used for cancer diagnosis.

Here, for the first time to our knowledge we demonstrate in principle that LIBS can be used for tissue analysis, specifically to differentiate between malignant and normal tissue. We analyzed malignant and normal tissue from a canine hemangiosarcoma

When this research was performed, the authors were with Mississippi State University, Mississippi State, Mississippi 39762: A. Kumar, F.-Y. Yueh, and J. P. Singh (singh@dial.msstate.edu), the Diagnostic Instrumentation and Analysis Laboratory, and S. Burgess, the College of Veterinary Medicine. A Kumar is now with the Department of Physics, College of Engineering, Architecture and Physical Sciences, Tuskegee University, Tuskegee, Alabama 36088.

Received 16 December 2003; revised manuscript received 22 June 2004; accepted 9 July 2004.

0003-6935/04/285399-05$15.00/0

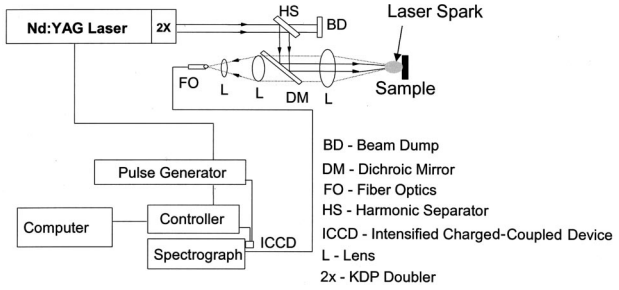

Fig. 1. Experimental diagram of the LIBS setup.

and show differences in elemental composition. Canine hemangiosarcoma, a model for human angiosarcoma, is a common incurable cancer of the hemopoetic system. Human angiosarcomas can be benign or malignant. However, because human angiosarcomas are rare, establishing criteria to diagnose whether they are malignant has been difficult. The canine hemangiosarcoma animal model may be valuable to define and analyze these types of tumor and suggest potential means of improving their classification in humans. LIBS provides rapid, nondestructive tissue analysis. LIBS analysis was also compared with the measurements with inductively coupled plasma emission spectroscopy (ICPES).

2. Experiment

A. Sample Preparation

Hemangiosarcoma and normal liver samples (1 cm × 1 cm × 2 cm) were taken from the liver of a dog. Each sample was bisected. One half of the sample (1 cm^3) was fixed in buffered formaldehyde saline [0.45% NaH_2PO_4, 0.55% Na_2HPO_4, 0.85% NaCl weight by volume (Sigma Aldrich, St. Louis, Missouri) and 10% formaldehyde (Fisher Scientific Co., Bridgewater, New Jersey)]. After a 48-h fixation, the tissues were then embedded in paraffin wax, sectioned, mounted, processed, and stained with hematoxylin and eosin as described.[21] The remaining half of the sample was placed in a drop of optimal cutting temperature embedding medium (BDH) on a square of Whatman filter paper (5 cm^2) and cooled in nitrogen vapor before immersion in liquid nitrogen. Sections (8 μm) were cut with a Cryocut cryostat (8 μm; Reichert-Jung), placed onto plain glass slides, and either air dried or air dried fixed in acetone (10 min). We also manually used thick-cut samples (~2 mm) taken directly from the tissue blocks.

B. Laser-Induced Breakdown Spectroscopy

The experimental arrangement of the LIBS system is shown in Fig. 1. A frequency-doubled Nd:YAG laser (Continuum Surelite III) was used in all measurements. The laser has a repetition rate of 10 Hz and a pulse width of 5 ns at 532 nm. An ultraviolet (UV) fused-silica lens was used to focus the laser beam to a spot size of approximately 0.04 mm. The same lens was used to collect light from the laser-induced spark. Two UV-grade quartz lenses were used to couple the LIBS signal to an optical fiber. The other end of the optical fiber was coupled to an UV–visible Echelle optical spectrograph (LLA Instruments, GmbH, ESA 3000 EV/I, Berlin, Germany) and used as an entrance slit. The spectrograph covers the 200–780-nm spectral range with a linear dispersion of approximately 5–19 pm/pixel. A 1024 X 1024-element intensified charge-coupled device (Kodak KAF-1001) with a pixel width of 0.024 mm cooled by Peltier elements was attached to the exit of the spectrograph and used to detect the light from the laser spark. We operated the detector in gated mode using a dedicated high-voltage fast-pulse generator (Stanford DG 535) that was synchronized to the laser output. We performed the data acquisition and analysis using a personal computer with ESAWIN software. To maximize the signal, the gate delay time and gate width were adjusted for each element to achieve the best signal-to-noise ratio data.

The LIBS setup was initially optimized with chicken blood samples, which were readily available. A thin layer of chicken blood was dried on a glass slide before the experiments. The laser beam was focused on the blood sample in such a way that the laser beam would ablate only the blood sample with no interference from the emission from air or the glass slide. This required a proper selection of laser energy and precise focusing. We selected a plano–convex quartz lens with a 7.5-cm focusing length to focus the laser beam on the sample. The selection of laser energy was also challenging. With very low laser energy (<10 mJ), the recorded data had a poor signal-to-noise ratio, and at high laser energy the strong background signal from the glass substrate caused a hindrance. Laser energy between 10 and 12 mJ produced good signal-to-background spectra from the blood sample. Before recording the LIBS signal of blood tissue on the glass plates, we used aluminum and Teflon thin plates as substrates. However, we could not eliminate the background signal from the substrate except in the case of glass. Glass was advantageous because it transmitted the unused laser light that was focused on the top of the thin layer of tissue cells. We recorded the LIBS spectra at different time delays and gate widths of the CCD detector and determined that the gate delay of 1 μs and the gate width of 10 μs were good for all the selected analyte lines in the 200–780-nm range. Figure 2 shows a typical LIBS spectrum from a chicken blood sample under the optimum experimental condition.

We used this optimized setup to record the LIBS spectra of normal and malignant tissues. In addition, we recorded the LIBS spectra of an ~2-mm-thick sample. The laser light was focused in such a way that only the ablation of the cells took place. The whole glass was mounted on a rotating pad, and the rotation of the pad was adjusted so that the laser light did not hit the same place more than once. We collected 20 individual frames of spectra in which each frame was the sum of spectra from ten laser

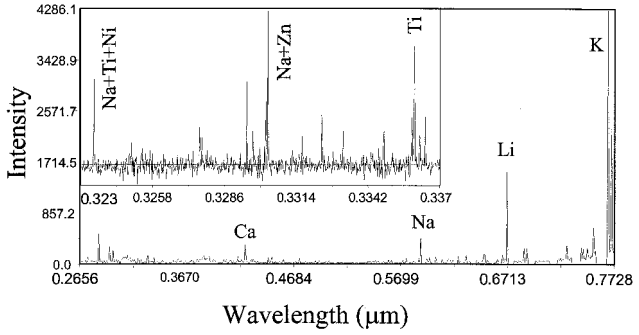

Fig. 2. LIBS spectrum of the blood sample of a chicken.

shots. Finally, the ten individual frames were averaged to obtain the resultant spectra.

C. Inductively Coupled Plasma Emission Spectroscopy

We analyzed the tissue samples by ICPES using a Perkin-Elmer Optima 4300 DV system. Dried tissue samples were initially dissolved in 10% HNO_3 + 1% HCl with the microwave digestion procedure. Finally, we purged the diluted samples in the plasma chamber using the argon gas. The system was already calibrated with the solutions of known concentrations of the different elements. The results of tissue analysis by ICPES are given in Table 1.

3. Results and Discussion

A. Laser-Induced Breakdown Spectroscopy Spectrum of Normal and Malignant Tissue Cells

Figure 3 shows the LIBS spectra of malignant and normal tissue cells at two spectral regions. There is a clear distinction between the spectra of normal and malignant tissue. The intensity of various elements, which is related to the concentration of trace elements in normal and malignant tissue, is significantly different. The elements identified from the LIBS spectra of tissue were Ca, Al, Fe, Cu, Na, K, and Mg. Many Fe lines were observed in these tissue spectra. The strongest Fe lines observed are 247.845, 296.69, 371.993, 385.99, 430.79, and 438.351 nm. The intensity of the Fe lines from malignant cells was weaker compared with the intensity from the normal cells. The lines of Ca were observed at 393.37, 396.85, 610.27, and 612.22 nm. The intensity of the Ca lines and the Al lines (394.4 and 396.15 nm) was found weaker than the malignant tissue cells. The lines of Na were observed at 589.0 and 589.6 nm. It was difficult to distinguish the tumor and normal cells on the Na lines alone because these resonant lines are easily self-saturated. Self-saturation is a phenomenon in spectroscopy when concentration of the atoms is too high and the line of emission is absorbed by the same kind of unexcited atoms that are in their ground state.

Table 1. Tissue Analysis by ICPES

Element	Analyte Line (nm)	Concentration (parts per million)	
		Normal Tissue	Malignant Tissue
Al	396.153	69.3 ± 0.69	56 ± 0.16
Ca	317.933	273 ± 1.81	410 ± 1.34
Cu	327.393	163 ± 0.89	12.4 ± 0.04
Fe	238.204	1820 ± 8.87	2110 ± 2.48
Mg	285.213	458 ± 2.56	420 ± 0.67
Na	589.592	2600 ± 9.71	9370 ± 29.94
K	766.490	5840 ± 28.83	5150 ± 11.65

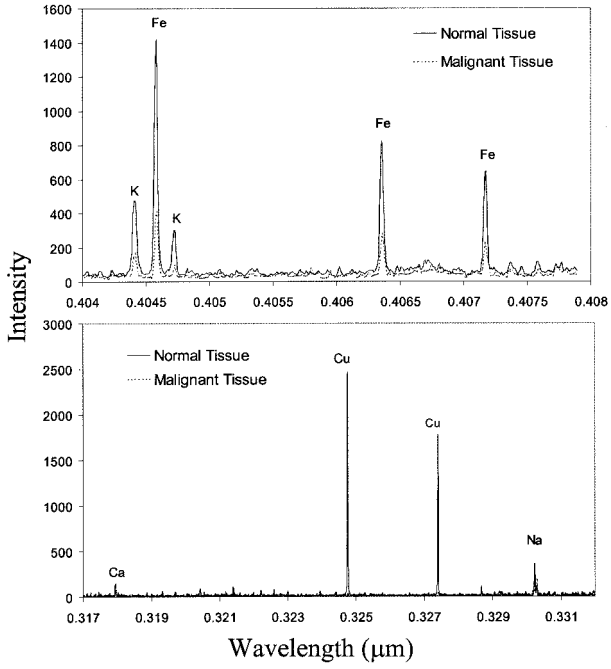

Fig. 3. LIBS spectra of the liver tissue of a dog in two different spectral regions.

Lines of Cu were observed at 324.754 and 327.396 nm (see Fig. 3). Cu lines are found to be much stronger in the normal tissue. However, we found no distinguishable differences in the LIBS spectra of the sections that were air dried only or the sections that were acetone fixed. The spectra recorded with thin tissue and a thick-cut sample were also compared. LIBS spectra from thin tissue shows a higher variation and a poorer signal-to-noise ratio compared with that from the thick-cut sample (Fig. 4). Therefore the results presented in Subsections 3.B and 3.C are from the data of the thick-cut sample.

B. Intensity Ratio

The intensity ratio of the major element with K at 766.491 nm was analyzed, and the results are shown in Table 2. The analyte lines selected for this calculation were the lines that give a better relative standard deviation. It is clear that the intensity ratios of Ca/K and Na/K are higher in the malignant tissue spectra. The Mg/K and Al/K are comparable in the normal and malignant tissue spectra, and Cu/K is lower in the malignant spectra. This indicates that the concentration of trace elements like Ca, Na, and Mg are higher in malignant cells in comparison with that in normal cells. Also, the concentration of Cu is

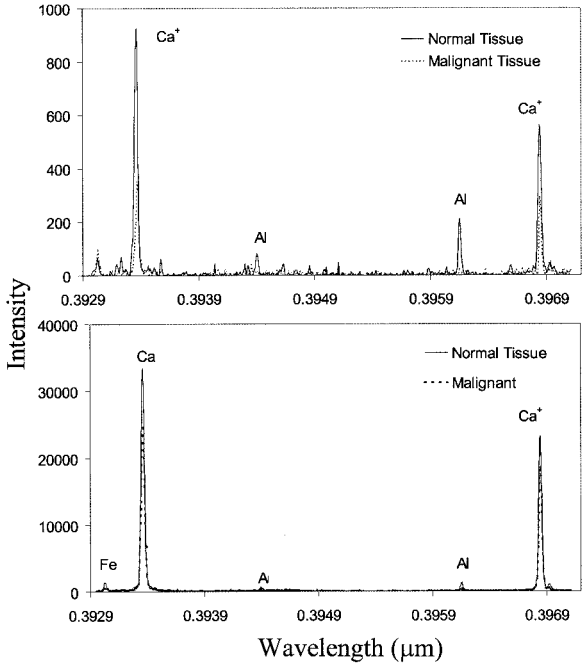

Fig. 4. LIBS spectra of tissue. Top, thin tissue; bottom, bulk tissue.

low in malignant cells in comparison with that in normal cells.

C. Comparison of the Results from Laser-Induced Breakdown Spectroscopy and Inductively Coupled Plasma Emission Spectroscopy

Because the LIBS system was not calibrated for different elements in the tissue, the intensity ratio obtained from LIBS was directly compared with the concentration ratio obtained from the ICPES measurements. This comparison is valid for optically thin laser-induced plasma because the intensity ratio is linearly proportional to the concentration ratio. The calculated ratios of the intensity ratios obtained from LIBS data of malignant tissue and normal tissue, with the concentration ratios obtained from ICPES analysis for malignant tissue and normal tissue, are listed in Table 3 and presented in Fig. 5. The LIBS data were in reasonable agreement with the ICPES data. The percentage difference between these two measurements was less than 12% for Al, Fe, Mg, and Na. The higher percent of difference for Cu and Ca might be due to the self-absorption effects. Because both the Cu and the Ca lines used in the LIBS analysis are resonant lines, the line intensity might not be linearly proportional to concentration due to self-absorption of these lines.

Table 2. Intensity Ratio from LIBS Spectra of Normal and Malignant Tissue

	Intensity Ratio	
Analyte Line (nm)	Normal Tissue	Malignant Tissue
Al 396.153/K 766.491	0.5919	0.49
Ca 396.847/K 766.491	12.77	31.42
Cu 327.39/K 766.491	1.45	0.07
Fe 430.791/K 766.491	0.73	1.03
Mg 279.551/K 766.491	3.37	3.62
Na 588.995/K 766.491	1.07	3.84

Table 3. Comparison of LIBS and ICPES Results

Elemental Ratio	Normal Tissue/Malignant Tissue		
	LIBS (I Ratio)	ICPES (C Ratio)	% Difference
Al/K	1.20	1.11	8
Ca/K	0.41	0.68	32
Cu/K	18.92	11.81	60
Fe/K	0.71	0.77	8
Mg/K	0.93	0.98	5
Na/K	0.28	0.25	12

I Ratio, intensity ratio; C Ratio, concentration ratio.

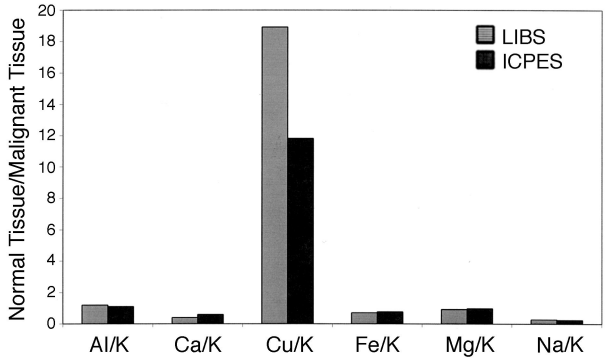

Fig. 5. Comparison of the Results of Tissue Analysis from LIBS and ICPES.

4. Conclusions

This is the first LIBS application to our knowledge to explore the possibility of using LIBS for cancer detection. In this study we have found the distinct difference in LIBS spectra of normal and malignant tissue in the spectral intensity distribution of the various elements in two types of sample. The line intensity ratios of different elements can be used to determine the concentration ratio of the trace elements in the tested tissue. From LIBS and ICPES data, we found that the concentration ratio of Ca, Cu, and Na with K is clearly different in normal and malignant samples. Although the result in this study is preliminary, it shows that LIBS has great potential for development as an *in vivo* diagnostic tool for cancer detection. Extensive development in this area is needed to obtain quantitative results for practical applications.

References

1. S. M. Hanash, "Biomedical applications of two-dimensional electrophoresis using immobilized pH gradients: current status," Electrophoresis **21,** 102–109 (2000).
2. J. B. Fenn, M. Mann, C. K. Meng, and S. F. Wang, "Electrospray ionization for mass spectroscopy of large biomolecules," Science **246,** 64–71 (1989).

3. F. Hillenkamp, M. Karas, R. C. Beavis, and B. T. Chait, "Matrix-assisted laser desorption and ionization mass spectrometry of biopolymers," Anal. Chem. **63,** 1193–1203 (1991).
4. M. Merchant and S. R. Weinburger, "Recent advances in surface-enhanced surface desorption/ionization–time of flight–mass spectrometry," Electrophoresis **21,** 1164–1167 (2000).
5. W. M. Kwiatek, T. Drewniak, M. Lekka, and A. Wajdowicz, "Investigation of trace elements in cancer kidney tissues by SRIXE and PIXE," Nucl. Instrum. Methods Phys. Res. B **109–110,** 284–288 (1996).
6. J. Hewlett, V. Nadeau, J. Ferguson, H. Moseley, S. Ibbotson, J. W. Allen, W. Sibbett, and M. Padgett, "The application of a compact multispectral imaging system with integrated excitation source to *in vivo* monitoring of fluorescence during topical photodynamic therapy of superficial skin cancers," Photochem. Photobiol. **73,** 278–282 (2001).
7. N. M. Ershaidat and S. H. Mahmood, "Elemental analysis of colorectal cancerous samples using XRF techniques," http://conference.kek.jp/JASS02/26_nidal.ppt.
8. F. Y. Yueh, J. P. Singh, and H. Zhang, "Elemental analysis with laser-induced breakdown spectroscopy," in *Encyclopedia of Analytical Chemistry* (Wiley, Chichester, UK, 2000).
9. D. A. Rusak, B. C. Castle, B. W. Smith, and J. D. Winefordner, "Fundamentals and applications of laser-induced breakdown spectroscopy," Crit. Rev. Anal. Chem. **27,** 257–290 (1997).
10. M. Z. Martin and M. D. Cheng, "The detection of chromium aerosol using time-resolved laser-induced plasma spectroscopy," Appl. Spectrosc. **54,** 1279–1285 (2000).
11. K. Song, Y.-I. Lee, and J. Sneddon, "Applications of laser-induced breakdown spectrometry," Appl. Spectrosc. Rev. **23,** 183–235 (1997).
12. B. J. Marquardt, S. R. Goode, and S. M. Angel, "*In-situ* determination of lead in paint by laser-induced breakdown spectroscopy using a fiber-optic probe," Anal. Chem. **68,** 977–981 (1996).
13. S. Morel, N. Leone, P. Adam, and J. Amouroux, "Detection of bacteria by time-resolved laser-induced breakdown spectroscopy," Appl. Opt. **42,** 6184–6191 (2003).
14. M. Corsi, G. Cristoforetti, M. Hidalgo, S. Legnaioli, V. Palleschi, A. Salvetti, E. Tognoni, and C. Vallebona, "Application of laser-induced breakdown spectroscopy technique to hair tissue mineral analysis," Appl. Opt. **42,** 6133–6137 (2003).
15. R. Bito, T. Shikano, and H. Kawabata, "Isolation and characterization of denatured serum albumin from rats with endotoxicosis," Biochim. Biophys. Acta **1646,** 100–111 (2003).
16. O. Samek, H. H. Telle, and D. C. Beddows, "Laser-induced breakdown spectroscopy: a tool for real-time, *in vitro* and *in vivo* identification of carious teeth," BMC Oral Health **1,** 1–9 (2001).
17. O. Samek, M. Liska, J. Kaiser, D. C. Beddows, H. H. Telle, and S. V. Kukhlevsky, "Clinical application of laser-induced breakdown spectroscopy to the analysis of teeth and dental materials," J. Clin. Laser Med. Surg. **18,** 281–289 (2000).
18. Q. Sun, M. Tran, B. Smith, and J. D. Winefordner, "*In-situ* evaluation of barrier-cream performance on human skin using laser-induced breakdown spectroscopy," Contact Dermatitis **43,** 259–263 (2000).
19. I. G. Pallikaris, H. S. Ginis, G. A. Kounis, D. Anglos, T. G. Papazoglou, and L. P. Naoumidis, "Corneal hydration monitored by laser-induced breakdown spectroscopy," J. Refract. Surg. **14,** 655–660 (1998).
20. A. C. Samuels, F. C. DeLucia, K. L. McNesby, and A. W. Miziolek, "Laser-induced breakdown spectroscopy of bacterial spores, molds, pollens, and protein: initial studies of discrimination potential," Appl. Opt. **42,** 6205–6209 (2003).
21. G. S. Pappas, *Laboratory Manual of Histology* (Brown, Dubuque, Iowa, 1990).